

Evolution of the magnetic domain structure of oriented 3% SiFe sheets with plastic strains

E. HUG

Division Matériaux, Laboratoire LG2MS (URA CNRS 1505), Département Génie Mécanique, Centre de Recherches de Royallieu Université de Technologie de Compiègne, BP649, 60206 Compiègne Cedex, France

Observations of the magnetic domain structure using a colloid method of strained grain oriented 3% SiFe alloy are reported. Density of the supplementary structure rises dramatically with small increases (about 2%) in plastic deformation. Transverse domain patterns suddenly appear around 4–5% of plastic strain. Close to the rupture of the alloy, zigzag lines and dissociation of main domain walls are observed. A statistical analysis of the different magnetic domain patterns has been made. An evolution in three distinct linear stages of the superficial densities of main and secondary structures is shown. Domain wall spacing of the main structure markedly decreases between 0 and 3% of strains and monotonous fall of domain wall spacing of the transverse patterns occurs. These experimental results establish that the transverse domain structure allows a compensation of the increase of the magnetoelastic energy that results from cold drawing of the alloy.

1. Introduction

Magnetic properties of materials are highly sensitive to lattice defects: non-magnetic inclusions, precipitates, dislocations, grain boundaries. In particular, strong alterations of magnetic characteristics are generated by plastic strains that result from the increase of the dislocation density and modifications of their configurations into the metallic matrix [1–6]. A change of the magnetic domain structure is therefore expected on account of the very large increase of the total magnetoelastic energy.

The observation of magnetic domains of ferromagnetic materials which contain a lot of dislocations remains very difficult and often limited to grain-oriented SiFe alloys which initially have a very small dispersion of the angular orientation of their grains. Weak misorientation of 180° domain configurations results.

The primary objective of this paper is to show several observations of magnetic domains on polycrystalline 3% SiFe oriented sheets which have undergone various cold drawing. The experimental procedure is given in Section 2. Section 3 describes the evolution of the magnetic domain patterns with plastic deformations. A statistical analysis of the different domain patterns is presented in Section 4. This allows us to show more precisely the influence of each class of domain walls on the magnetic degradation process. A discussion of our different outcomes is reported in Section 5.

2. Experimental procedure

2.1. Working out of the colloidal solution

The Bitter figure technique was the first method used to visualize magnetic domains of materials. It is still used today [7–9] because it is the simplest method as far as equipment is concerned.

The colloid solution was prepared using the methods of Elmore [10] and Bitter [11]. The first stage is the production of magnetite Fe_3O_4 by the Lefort method; a solution of 2 g $\text{FeCl}_2 \cdot 4\text{H}_2\text{O}$ and 5.4 g $\text{FeCl}_3 \cdot 6\text{H}_2\text{O}$ in 300 cm^3 is heated and stirred. Sodium hydroxide solution (5 g in 50 cm^3 H_2O) is then added drop by drop to product a heavy and black precipitate of magnetite. Next, this precipitate is filtered off and washed in distilled water. The filtrate is then washed using 0.01 N HCl and added to a solution of sodium oleate and distilled water (Elmore's method). The quantity of water varies between 300 cm^3 and 1 l for more and less diluted colloidal solutions. The pH of the solution is an important parameter. Indeed, Garrod pointed out that a critical point does exist on the graph of mobility of particles = $f(\text{pH})$. Stability of the solution is obtained for $\text{pH} \leq 5.2$ [12]. Dispersion of the solution is eventually obtained by ultrasonic agitation.

The colloidal solution which contains particles of all sizes must be filtered. It gives good results but needs to be regularly activated using a strong magnetic field strength or an adequate boiling method.

2.2. Preparation of specimens for the study of domain patterns

Specimens of $20 \times 10 \text{ mm}^2$ were cut in the centre of plastically deformed samples of grain-oriented 3% SiFe. The sheet studied was 0.35 mm thick. The samples were all stressed along the rolling direction. To avoid introduction of internal stresses into the die and the obtention of "maze patterns" [13], an acid etch (HF + HCl) was followed directly by electropolishing with the acid solution: 700 ml ethanol + 120 ml distilled water + 100 ml glycerol + 80 ml perchloric acid [14]. A stainless steel cathode is used and a potential at about 30 V is applied. The time of electropolishing is 30 s on average.

2.3. Obtention of magnetic domain patterns

The formation of a thin layer of colloid between the surface of the alloy and a cover slip is obtained

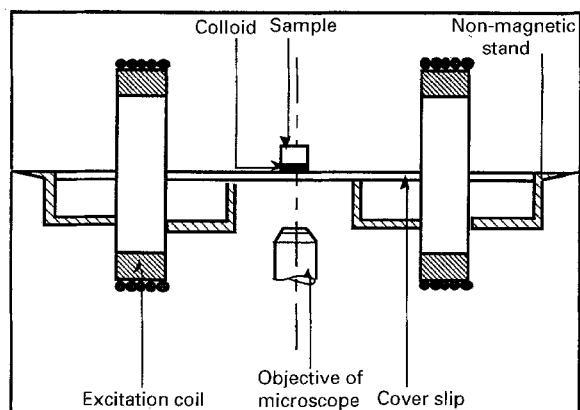


Figure 1 Magnetization apparatus for the observation of magnetic domains.

through a few drops of the solution. Patterns may be visualized using an optical metallurgical microscope. Specimens can be submitted to a d.c. magnetization, whose field strength range from 0 to 800 A m^{-1} . A schematic illustration of the magnetization equipment is shown in Fig. 1. The directions of magnetization in domains are determined using the method of "striations of colloid" [15] and a scratch technique [15, 16]. Scratches are obtained with the diamond of a microhardness apparatus, before electropolishing of samples.

3. Evolution of magnetic domain patterns of oriented 3% SiFe alloys with plastic deformations

Figs 2 to 8 show the evolution of magnetic domain structure for the oriented 3% SiFe alloy, with increasing plastic strains.

3.1. Initial configuration of magnetic domain structure

The configurations of magnetic domains more frequently observed on non-deformed samples are illustrated in Figs 2, 3 and 4. Basic patterns consist of boundaries of 180° domains roughly parallel to the easy direction $\langle 001 \rangle$ (slab domains or main domains, Fig. 2). Grain-oriented sheets have a theoretic Goss texture $\{110\} \langle 001 \rangle$. In fact some weak misorientation does exist so 180° boundaries are slightly misoriented with respect to the rolling direction. 180° domains are often continuous across grain boundaries, or reverse spikes of opposite magnetization are created (Fig. 4). We also observed lancet networks in slab domains for more misoriented grains (Fig. 3).

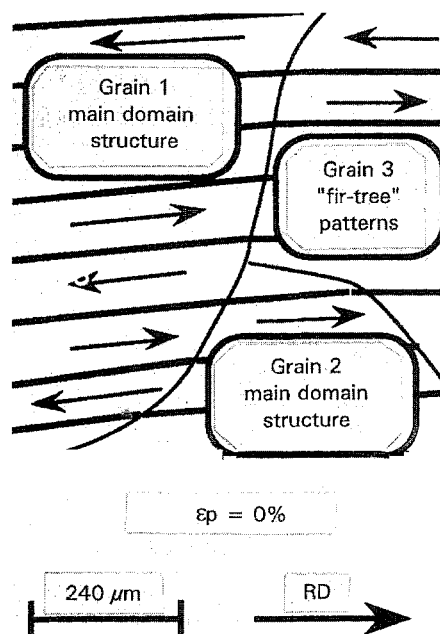
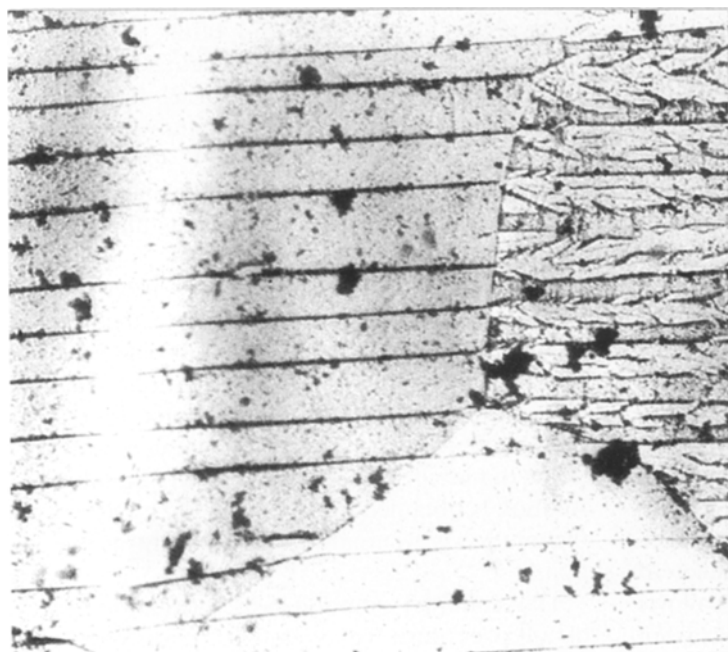


Figure 2 Magnetic domain structure of unstrained grain-oriented 3% SiFe. Slab domains and "fir-tree" patterns (arrows indicate direction of magnetization into domains, RD: rolling direction).

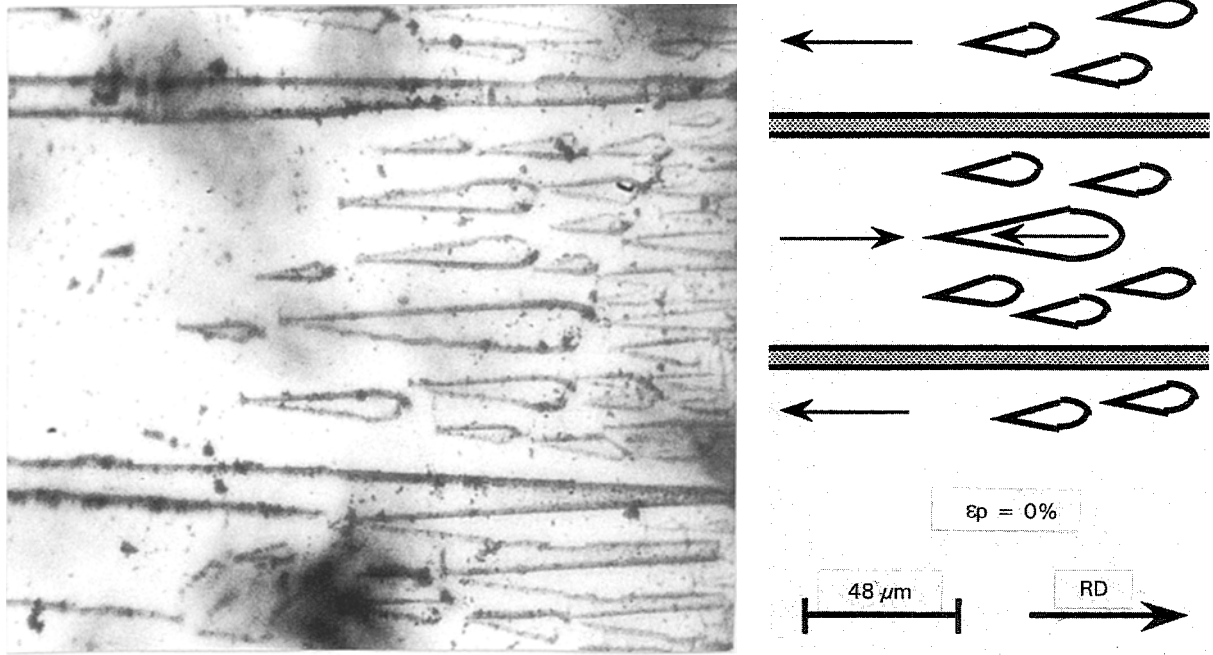


Figure 3 Magnetic domain structure of unstrained grain-oriented 3% SiFe. Lancet network into main domain structure is shown.

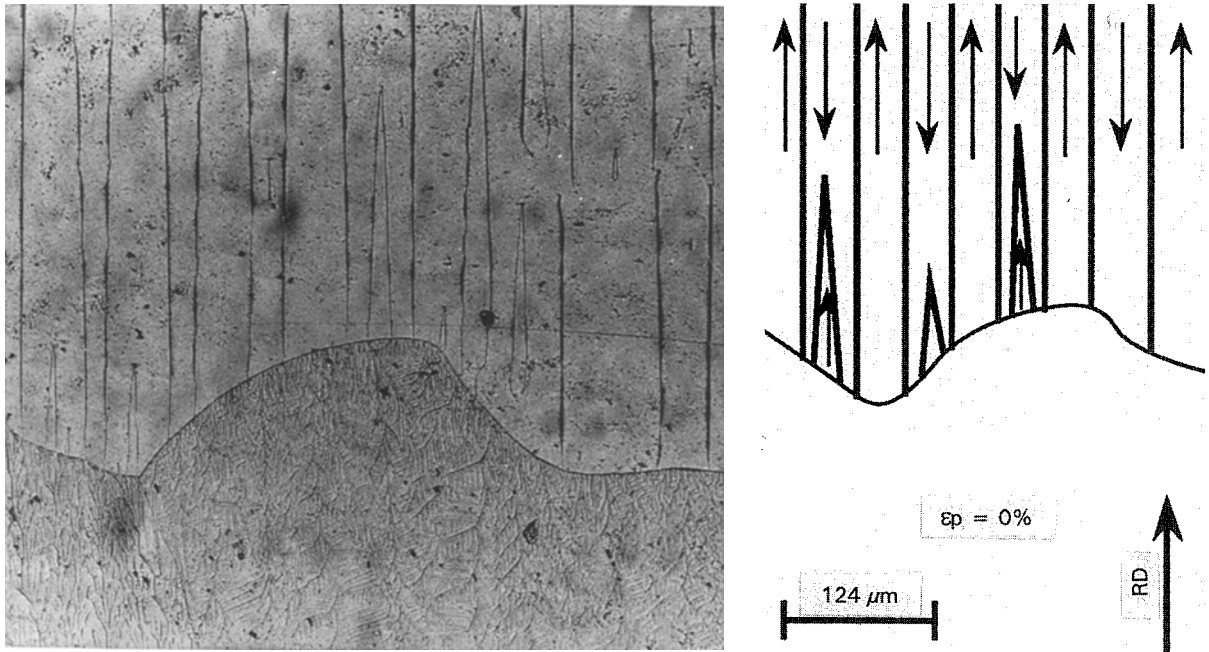


Figure 4 Magnetic domain structure of unstrained grain-oriented 3% SiFe. Main domains and reverse spikes of opposite magnetization on a grain boundary are shown.

Such domain patterns (reverse spikes and lancets) we term “secondary domain structures”.

Here and there, strongly disrupted domain configurations appear which are impossible to identify with our experimental device. We will call these patterns “chaotic domain structures”. These are few in number for undeformed samples.

3.2. Evolution of the magnetic domain structure with plastic deformations

When the plastic deformation ϵ_p ranges from 0 to 2%, the density of the supplementary structure rises dramatically. Furthermore, strongly perturbed domain patterns can be seen next to grain boundaries (Fig. 5). 180° walls are more and more misoriented across

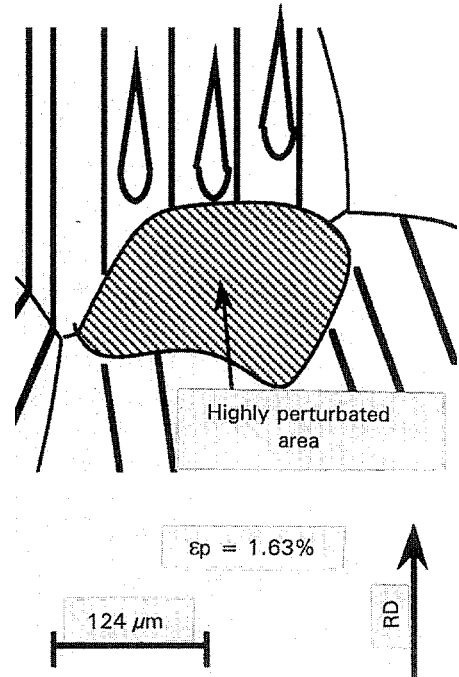
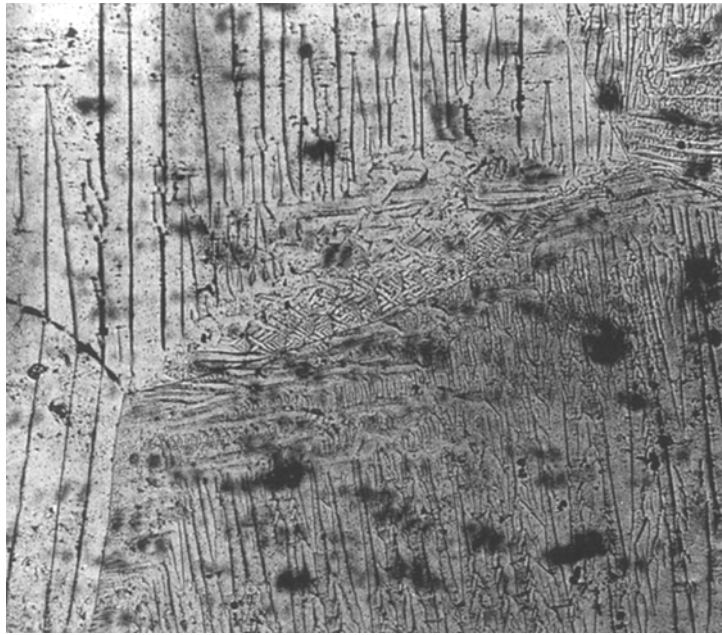


Figure 5 Magnetic domain structure of strained grain-oriented 3% SiFe. Degradation of magnetic domain patterns close to a grain boundary and formation of a “chaotic” domain structure are shown.

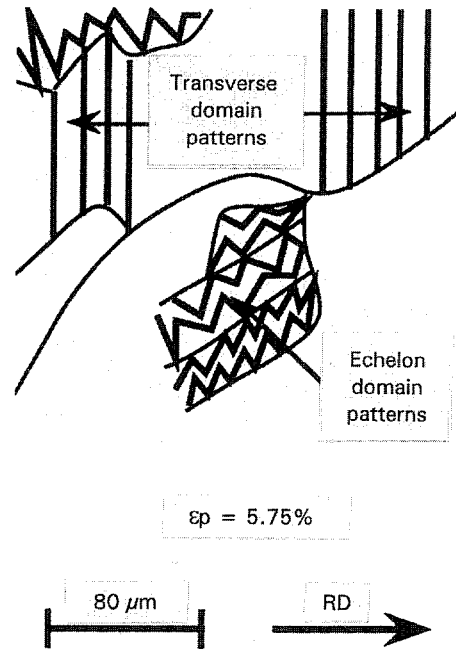
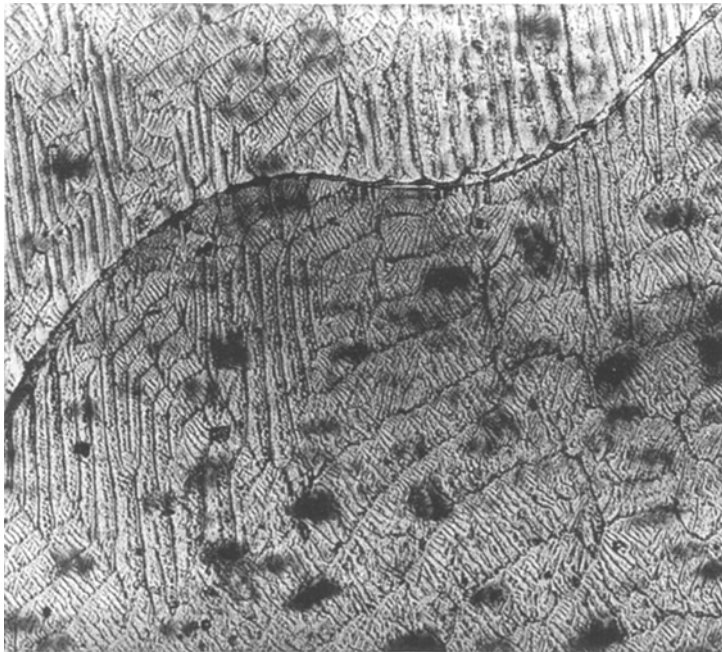


Figure 6 Magnetic domain structure of strained grain-oriented 3% SiFe showing transverse domain patterns and echelon structure.

grain boundaries. Around 4–5% of plastic strains, the 180° walls are frequently decorated by “fir-tree” patterns. These domains minimize the density of free poles on the surface of the sample. Transverse domains also become visible at some grain boundaries (Fig. 6). This last structure also appears suddenly into slab domains (Fig. 7) but 180° domain walls remain linear as far as the grain boundaries. Bowing of main domain walls across grain boundaries is observed beyond $\epsilon_p = 8\%$.

Close to the rupture of the samples, this bowing tends to propagate itself along all the length of 180° domain walls. On fractured test pieces, three classes of magnetic domains may be recognized: transverse domains which can exist in all the area of grains (Fig. 8); zigzag lines and “λ-domain structure” [17] at grain boundaries (Fig. 9); bowing of slab domain walls occurring on the total surface of several grains (Fig. 10). This last phenomenon is due to the strong pinning power of dislocation tangles which exist at this rate of

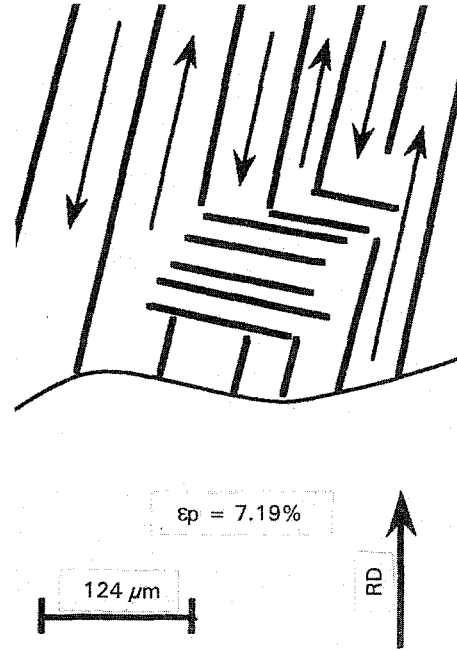
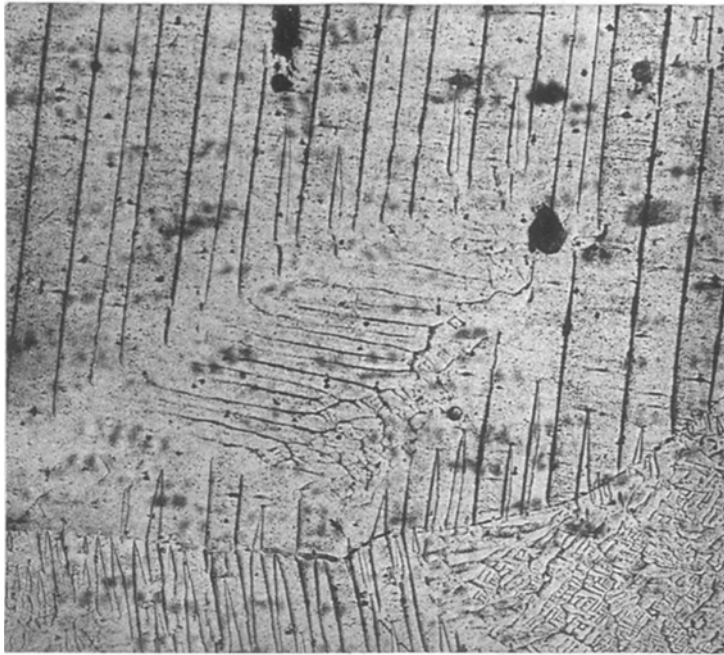


Figure 7 Magnetic domain structure of strained grain-oriented 3% SiFe showing a transverse domain pattern which suddenly appears into the main domain structure.

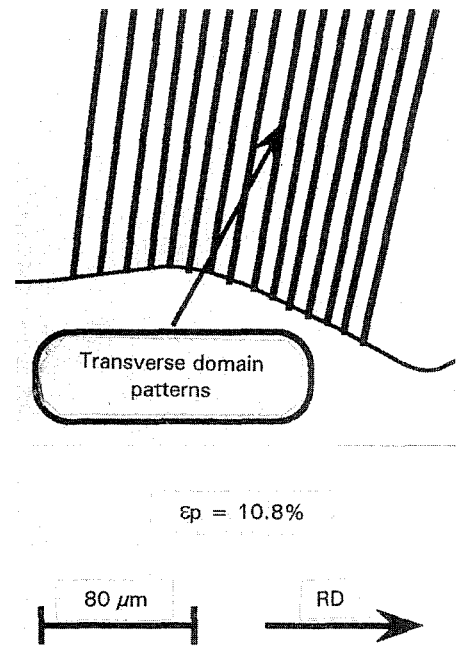
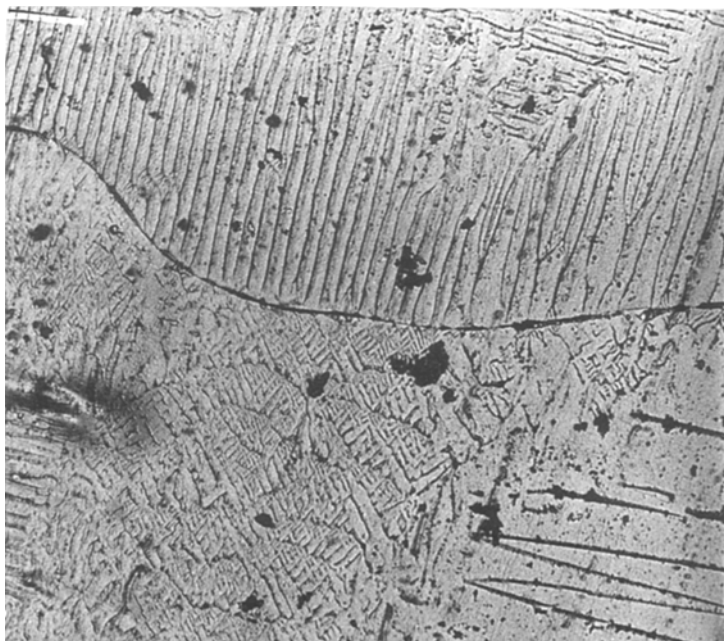


Figure 8 Magnetic domain structure of fractured grain-oriented 3% SiFe. Transverse domain patterns covering the total area of a grain are shown.

deformation. The density of the main domain structure which is not affected by cold drawing is approximately 8% of the investigated surface.

4. Statistical analysis of the magnetic domain patterns observed on strained grain-oriented 3% SiFe

4.1. Methodology

In an attempt to better understand the magnetoelastic coupling inside the ferromagnetic alloy studied, a statistical analysis of the magnetic domain structures observed has been realized. To this end, we may define these representative parameters:

istical analysis of the magnetic domain structures observed has been realized. To this end, we may define these representative parameters:

- D_{moy} : domain wall spacing for main domain structures;
- D_{tr} : domain wall spacing for transverse domain structures;
- Ω_1, Ω_2 : medium superficial density of main and secondary domain structures, respectively,

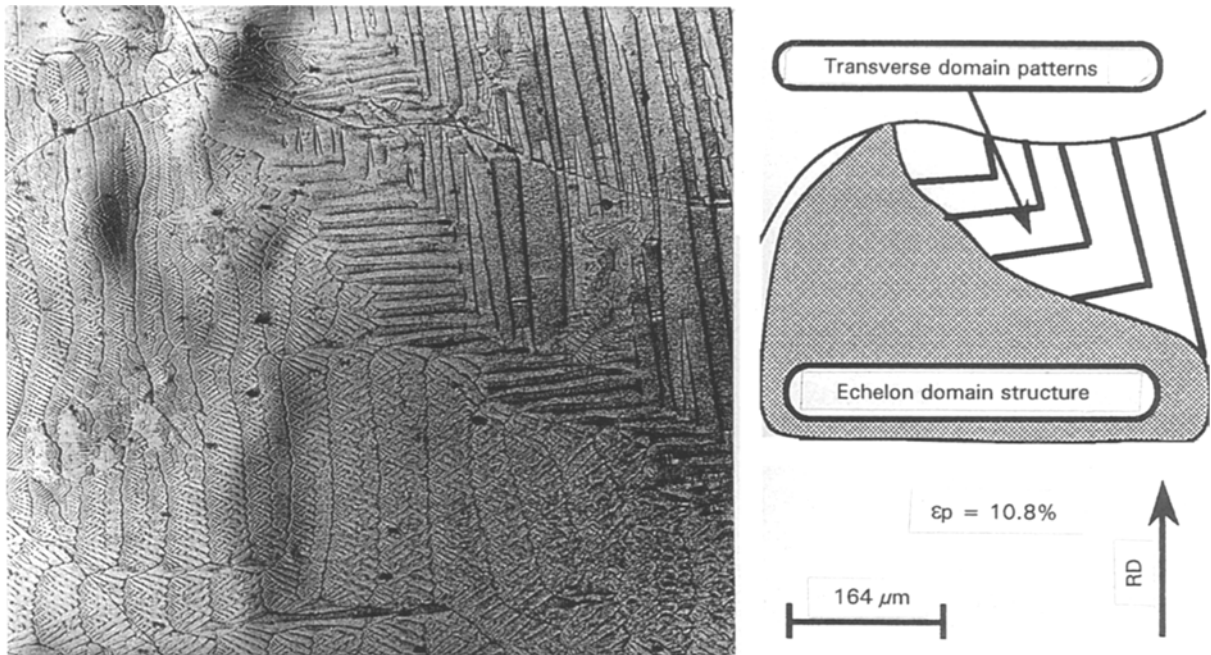


Figure 9 Magnetic domain structure of fractured grain-oriented 3% SiFe showing transverse domains and echelon patterns.

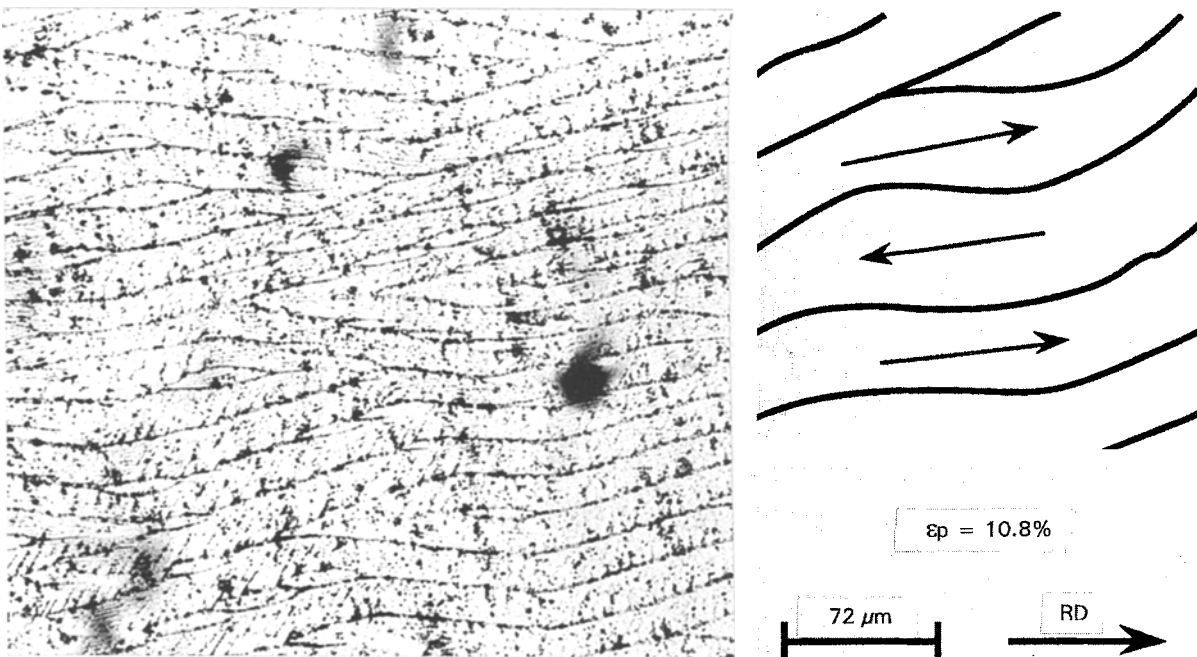


Figure 10 Magnetic domain structure of fractured grain-oriented 3% SiFe. This shows the zigzag of main 180° boundary walls under the strong pinning effect of the tangles of dislocations.

according to Shilling and Houze's terminology [18].

Domain wall spacing is a function of the length of grains [19, 20]. Consequently, D_{moy} and D_{ir} have been measured on grains of similar diameters. The densities of domain structures have been shaken using a computer imaging analysis. Results are given as a function of the total investigated surface.

4.2. Experimental results

4.2.1. Superficial densities Ω_1 and Ω_2

An examination of unstrained grain-oriented 3%SiFe samples shows that main domain structure appears at about 65% of the investigated surface. The other 35% contains reverse spikes and a lancet network. A few grains of small diameter exhibit a chaotic domain structure. Neither transverse domains nor echelon patterns appear.

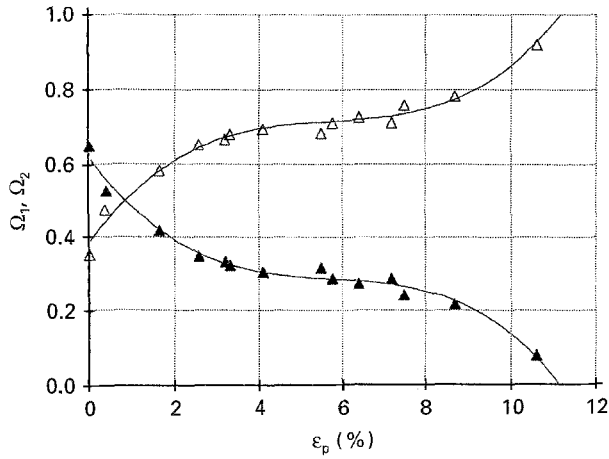


Figure 11 Variation of the densities of main and secondary domain structures as a function of plastic strains. \blacktriangle Ω_1 ; \triangle Ω_2 .

For ε_p ranging from 0 to 2%, Ω_1 decreases markedly to 37% of the total observed area. The flux closure domain walls are essentially reverse spikes and greatly perturbed zones at grain boundaries, constituted of echelon structures.

Transverse domains suddenly appear around 3% of plastic deformation. Furthermore, we also notice a relative stabilization of Ω_1 and Ω_2 after this strain rate. For ultimate values of deformations, Ω_2 increases again at the expense of Ω_1 because bowing of slab walls occurs. Ω_1 reaches 8% of the total area for the fractured samples.

The course of Ω_1 and Ω_2 with ε_p is shown graphically in Fig. 11. Plastic deformation of the alloy causes a variation of superficial densities of magnetic domains in three distinct linear stages:

- Important degradation of the magnetic structure for $\varepsilon_p \in 0-3\%$;
- Stabilization of the superficial densities between 3 and 8%;
- Bowing of 180° domain walls which again cause a destruction of magnetic structure beyond $\varepsilon_p = 8\%$.

4.2.2. Domain wall spacings D_{moy} and D_{tr}

Plotting D_{moy} and D_{tr} against ε_p shows the same trend as before (Fig. 12). Domain wall spacing for the main domain structure strongly decreases between 0 and 3% ($73 \mu\text{m}$ for $\varepsilon_p = 0\%$; $40 \mu\text{m}$ for $\varepsilon_p = 3.5\%$). Beyond 3–4% of plastic strain, a relative stagnation of D_{moy} occurs.

On the other hand, transverse domains suddenly appear with an initial domain wall spacing of magnitude $D_{tr} = 33 \mu\text{m}$. Monotonous decrease of D_{tr} then occurs up to a final value of $10 \mu\text{m}$.

5. Discussion

Variations of the representative parameters of the microscopic magnetic state of grain-oriented 3%SiFe, as illustrated in Figs 11 and 12, must be considered as general tendencies. Measurements of D_{moy} , D_{tr} , Ω_1 and Ω_2 has been made on about 50 grains for each defor-

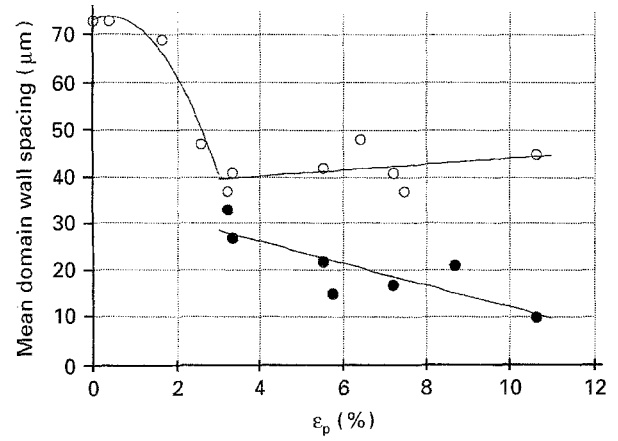


Figure 12 Variation of the domain wall spacing for main and transverse domain structures as a function of plastic strains. \circ D_{moy} ; \bullet D_{tr} .

mation rate. These grains have been chosen as the more representative of the magnetic domain state of the samples.

D_{moy} and D_{tr} are mean values of a hundred experimental measurements for each strain rate. Likewise, the two densities Ω_1 and Ω_2 are mean values of 50 measurements. Furthermore, D_{moy} and D_{tr} are distributed according to a Gaussian statistical law but Ω_1 and Ω_2 strongly fluctuate around their mean values.

Consequently, D_{moy} and D_{tr} are the more representative parameters of the micromagnetic state of the samples. Ω_1 and Ω_2 just give us qualitative information about the repartitions of the different magnetic domain structures on the surface of the samples.

Nevertheless, these experimental results show the importance of transverse domain structures. These domains try to compensate for the increase of magnetoelastic energy due to the cold drawing of the material. Their sudden creation around 3% of plastic deformation implies the relative stabilization of the density of flux closure domain patterns. As we have shown elsewhere, magnetic properties of oriented SiFe alloys (magnetization curve, coercive strength and core losses) are then less sensitive to plastic deformation [2].

The metallurgical state of the material between 0 and 0.5% of plastic strains is characterized by the Lüders strain state, which involves an important heterogeneous dislocation structure inside the metal die. After this, dislocation structure remains more or less homogeneous up to 8% strain (small tangles and isolated dislocations). These two dislocation structures are the more harmful for the magnetic properties of the alloys. From $\varepsilon_p = 8\%$ to the rupture, dislocation configuration becomes progressively inhomogeneous and walls of high density are created but any supplementary magnetic damage is observed [21].

The strong degradation of magnetic properties of the 3% SiFe alloys occurring in the first stage of plastic deformation can therefore be related to the increasing of the density of the spike domains due to the structure of the dislocations at the Lüders state.

6. Conclusion

The domain patterns of grain-oriented 3% SiFe alloys submitted to various plastic strains have been observed. We state the following conclusions in view of our experimental results:

1. The main domain structure constitutes about 65% of the investigated surface of unstrained specimens. The other part contains reverse spikes and lancet network. Neither transverse domains nor echelon patterns appear.
2. For plastic deformation ranging from 0 to 2%, the density of the main domain structure decreases markedly to 37% of the total observed area. Flux closure domains are essentially reverse spikes, lancet networks and greatly perturbed zones at grain boundaries, constituted of echelon structures.
3. Transverse domains suddenly appear around 3% of plastic deformation. As a result, stagnation of the density of main and secondary domain structures occurs. These patterns compensate for the increase of magnetoelastic energy due to cold drawing of the material. This results in relative stabilization of the densities of the flux closure domain patterns.
4. For plastic deformations close to the rupture of the material, the density of the secondary structure still increases at the expense of the density of the slab domains. Few unaffected main domains are visible on the fractured samples because a bowing of 180° main domain walls occurs.

The observation of the domain structure of strained specimen then gives some indications about the texture of cold drawing which appears during plastic deformation and about the resulting residual stress state of the alloy. More work needs to be done in this area. Nevertheless, continuing research may provide more understanding about the degradations of magnetic properties, especially energy losses, in laminated cores of electromechanical systems during manufacture.

Acknowledgements

The author is deeply grateful to Professors M. Kant (Division électromécanique, UTC, Compiègne) and

M. Clavel (Division Mécanique, UTC, Compiègne) for their kind help in the course of this research. The author also wants to express his appreciation to Professor Degauque (Laboratoire de Physique des Solides, INSA, Toulouse) for making several useful remarks.

References

1. P. W. NEURATH, *J. Met. Trans. AIME* (1956) 1319.
2. E. HUG, Thesis, University of Compiègne (1993).
3. F. DUMAS, E. HUG, M. CLAVEL and J. L. ILLE, *J. Phys. IV* **2** (1992) 47.
4. E. HUG, F. DUMAS, J. M. BIEDINGER and M. CLAVEL, *Rev. Metal. CIT/Sc., Gen. Mat.* (12) (1994) 1857.
5. J. DEGAUQUE, B. ASTIE and L. P. KUBIN, *Phys. Stat. Sol.* **45(a)** (1978) 493.
6. *Idem.*, *J. Appl. Phys.* **50(3)** (1979) 2140.
7. K. MOHRI, S. I. TAKEUCHI and T. FUJIMOTO, *IEEE Trans. Mag.* **15(5)** (1979) 1346.
8. *Idem.*, *Ibid.* **15(6)** (1979) 1598.
9. *Idem.*, *Mem. Kyushu Inst. Technol.* (1988) 9.
10. W. C. ELMORE, *Phys. Rev.* **54** (1938) 309.
11. F. BITTER, *Ibid.* **38** (1931) 1903.
12. J. R. GARROOD, *Proc. Phys. Soc.* **79** (1962) 1252.
13. R. CAREY and E. D. ISAAC, "Magnetic domains and techniques for their observation" (English Universities Press, London, 1966).
14. W. J. McG. TEGART, "Polissage électrolytique et chimique des métaux au laboratoire et dans l'industrie" (Dunod, Paris, 1960).
15. H. J. WILLIAMS, R. M. BOZORTH and W. SHOCKLEY, *Phys. Rev.* **71(1)** (1949) 155.
16. H. J. WILLIAMS, *Ibid.* **71** (1947) 646.
17. Y. LUO, Z. WANG and H. PFUTZNER, *J. Mag. Mag. Mat.* **41** (1984) 17.
18. J. W. SHILLING and G. L. HOUZE Jr, *IEEE Trans. Mag.* **10(2)** (1974) 195.
19. D. J. CRAIK and R. S. TEBBLE, "Ferromagnetism and ferromagnetic domains" (North-Holland Publishing Company, 1965).
20. L. F. BATES and C. D. MEE, *Proc. Phys. Soc.* **65** (1951) 129.
21. E. HUG, M. KANT and M. CLAVEL, *J. Phys. III* **4** (1994) 1267.

Received 6 June 1994

and accepted 22 March 1995